

Dispersion and Band-Gap Scaling of the Electronic Kerr Effect in Solids Associated with Two-Photon Absorption

M. Sheik-Bahae, D. J. Hagan,^(a) and E. W. Van Stryland^(b)

Center for Research in Electro-Optics and Lasers (CREOL), University of Central Florida, Orlando, Florida 32816

(Received 1 December 1989)

Measurements of the nonlinear refractive index using beam-distortion methods and four-wave mixing show a strong systematic dispersion in the bound-electronic nonlinearity (electronic Kerr effect n_2) near the two-photon-absorption edge. We find that with the two-photon-absorption spectrum predicted by a two-parabolic-band model, we can predict the observed universal dispersion, scaling, and values of n_2 that range over 4 orders of magnitude and change sign, using a simple Kramers-Kronig analysis. The resulting scaling rule correctly predicts the value of n_2 for 26 different materials, including wide-gap dielectrics and semiconductors.

PACS numbers: 78.20.Wc, 42.65.Bp, 42.65.Jx

The study of nonlinear optics in semiconductors has primarily concentrated on band-gap-resonant effects. The very large nonlinear effects observed in this case are the saturation of interband and excitonic absorption due to photoexcited free carriers and excitons, and the associated negative change in the refractive index. In contrast, by exciting optical solids at frequencies much less than the gap, a considerably smaller and faster, positive nonlinear refractive index (n_2) due to bound-electronic effects is observed. This n_2 arises from the real part of the third-order susceptibility $\chi^{(3)}$ and is defined through the refractive index change Δn , where

$$\Delta n(\omega) = \gamma(\omega)I_\omega = \frac{1}{2}n_2(\omega)|E_\omega|^2, \quad (1)$$

with I_ω and E_ω being the irradiance and electric field at frequency ω , respectively, and $n_2 = (2\pi/n_0)\text{Re}\{\chi^{(3)}\}$. The linear refractive index is n_0 , and γ and n_2 are related by $n_2(\text{esu}) = (cn_0\gamma/40\pi)(\text{mks})$, where c is the speed of light. The magnitude and dispersion of n_2 is of interest because of its importance in applications such as nonlinear propagation in fibers, fast optical switching, self-focusing and damage in optical materials, and optical limiting in semiconductors.

Most studies of n_2 in optical solids usually concentrate on wavelengths far below the energy gap (E_g). However, recently we found that measurements in semiconductors substantially above the two-photon-absorption (2PA) edge ($E_g/2$) yield negative values for n_2 .¹ We have extended these measurements to a large number of other materials including semiconductors and dielectrics above and below the 2PA edge. As a result, we have been able to clearly demonstrate the behavior of the dispersion of n_2 .

Utilizing a newly developed technique (Z scan) for n_2 measurements^{1,2} that can determine its magnitude and sign, we have measured n_2 for several semiconductors and wide-gap dielectrics at 1.064 and 0.532 μm . This simple technique has been shown to be an accurate and sensitive tool for measuring n_2 even in the presence of

nonlinear absorption. For example, we find a negative n_2 in materials such as ZnSe at 0.532 μm where 2PA is present, but find that the sign changes at 1.064 μm . We have also performed picosecond, degenerate, four-wave-mixing (DFWM) measurements which show this third-order response to be fast (time-resolution limited by the 30-ps pulse width) and dominant at irradiances up to $\approx 0.5 \text{ GW/cm}^2$, while at higher irradiances the slowly decaying 2PA-generated free-carrier refraction becomes important.³ DFWM studies in other semiconductors and other wavelengths show this to be a universal phenomenon.

It has previously been predicted that $\chi^{(3)}$ should vary as E_g^{-4} .^{4,5} Using this scaling and the relation between n_2 and $\chi^{(3)}$ that includes the linear index n_0 , we can remove the E_g and n_0 dependences from the experimental values of n_2 by multiplying them by $n_0E_g^4$. Figure 1 shows a plot of our experimentally determined scaled values of n_2 as a function of $\hbar\omega/E_g$. We also divide the data by a constant K' which we explain in what follows. We show on the same plot several data for large-gap optical crystals obtained from recent measurements by Adair, Chase, and Payne using a "nearly degenerate three-wave-mixing" scheme.⁶ Our own measurements of several of the same materials studied in Ref. 6 show excellent absolute agreement. Assuming that there are no other relevant parameters unique to each material other than band gap and index, this plot should be general to all optical solids. Upon examination of Fig. 1 we immediately see a trend giving small positive values for low ratios of photon energy to band-gap energy which slowly rises to a broad resonance peak at the 2PA edge and then decreases, eventually turning negative between the two-photon- and single-photon-absorption edges. We should note that the scaling with E_g hides a variation in magnitude of n_2 of 4 orders of magnitude so that the observed universal dispersion curve is quite remarkable. This dispersion curve is qualitatively similar to the dispersion of the linear index around the single-photon-

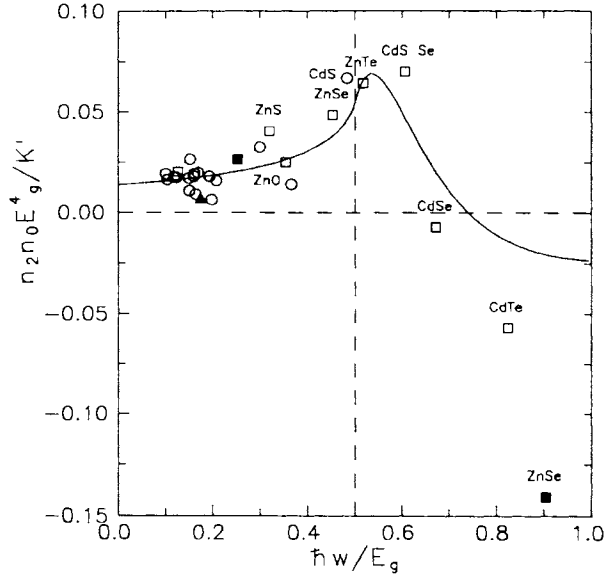


FIG. 1. Data of n_2 scaled as $n_2 n_0 E_g^4 / K'$ vs $\hbar \omega / E_g$. The open circles represent the data from Ref. 6 all obtained at $\lambda = 1.06 \mu\text{m}$. The remaining data are our measurements using the Z-scan technique taken at $\lambda = 1.06 \mu\text{m}$ (open squares), at $\lambda = 0.532 \mu\text{m}$ (solid squares), and at $\lambda = 10.6 \mu\text{m}$ (solid triangle). Only the semiconductor data within the highly dispersive region are labeled for comparison. The solid line is the calculated dispersion function G_2 with no adjustable parameters.

absorption edge.⁷ As these linear quantities are related by causality via a Kramers-Kronig (KK) relation, it seems logical to investigate whether the observed dispersion of n_2 can be calculated using a nonlinear Kramers-Kronig relation between the real and imaginary parts of $\chi^{(3)}$. Indeed, as we will show, making some reasonable assumptions, the observed tendencies as well as the absolute magnitudes of this dispersion are well predicted by such a calculation. Figure 1 is the direct result of such a calculation including only the 2PA contribution to the imaginary part of $\chi^{(3)}$. The 2PA spectral dependence is well established both experimentally and theoretically.⁸⁻¹¹ It should be noted that no fitting parameter is used in this calculation, which is presented below.

Most theoretical calculations of n_2 have been confined to the zero-frequency limit.¹²⁻¹⁶ Of these, semiempirical formulations have been most successful in predicting the magnitude of n_2 .^{15,16} For example, the formula obtained by Boling, Glass, and Owyong in relating n_2 to the linear index (n_0) and the dispersion of n_0 in terms of the Abbe number has been successfully applied to a large class of transparent materials.^{6,16} Their theory predicts the low-frequency magnitude of n_2 , but does not give the dispersion. The KK method described here predicts the dispersion as well as the magnitude of n_2 . This calculation assumes that 2PA gives the dominant contribution to n_2 and that other contributions from electronic Raman and the ac Stark effect ("virtual band blocking")

are ignored. We will return to this assumption later.

Based on the principle of causality, the KK transformation states that a change in the refractive index (Δn) at ω is associated with changes in the absorption coefficient ($\Delta \alpha$) throughout the spectrum (ω') and vice versa. We write this as

$$\Delta n(\omega; \xi) = \frac{c}{\pi} \int_0^\infty \frac{\Delta \alpha(\omega'; \xi)}{\omega^2 - \omega'^2} d\omega', \quad (2)$$

where c is the velocity of light in vacuum and ξ is a parameter (or parameters) denoting the "cause" of change in the absorption. The cause need not be of optical origin but could be any external perturbation, such as thermal excitation, etc. For cases where an electron-hole plasma is injected, the consequent change of absorption has been used to obtain the plasma contribution to the refractive index. In this case, the ξ parameter is taken as the change in plasma density (ΔN) regardless of the mechanism of generation of the plasma or the pump frequency.¹⁷ In the case of 2PA the change is due to the presence of a pump field at Ω (i.e., $\xi = \Omega$). The corresponding nonlinear refraction is $\Delta n(\omega, \Omega)$, which gives the dispersion of the index change with ω . For the case of self-refraction, $\omega = \Omega$, and this gives what is commonly referred to as n_2 . Van Vechten and Aspnes¹⁴ obtained the low-frequency limit of n_2 from a similar KK transformation of the Franz-Keldysh electroabsorption effect where, in this case ξ is the dc field. The bound-electronic contribution to $\chi^{(3)}$ can originate from various absorptive counterparts that are quadratic functions of the pump field. Effects of this order may include 2PA, the electronic Raman effect, and the optical Stark effect. Here we consider only 2PA.

A wealth of experimental and theoretical work regarding 2PA in semiconductors and crystalline materials exists. In accordance with the predictions derived from either a second-order perturbation calculation of the transition rate^{5,8} or a Keldysh-type formalism,⁹ the 2PA coefficients of the semiconductors studied in Ref. 10 were found to be in good agreement with the theoretical expression given as

$$\beta(2\omega') = K \frac{\sqrt{E_p}}{n_0^2 E_g^3} F_2 \left(\frac{2\hbar\omega'}{E_g} \right), \quad (3)$$

where K is a material-independent constant and E_p (related to the Kane momentum parameter, a momentum matrix element) is nearly material independent and possesses a value of ≈ 21 eV for most direct-gap semiconductors. Note that $\beta = (4\pi\omega/n_0) \text{Im}\{\chi^{(3)}\}$. The function F_2 is only a function of the ratio of the photon energy $\hbar\omega'$ to E_g (i.e., the optically coupled states). The functional form of F_2 reflects the assumed band structure and the intermediate states considered in calculating the 2PA transition rate. The simplest model assumes a pair of isotropic and parabolic bands and intermediate states that are degenerate to initial (valence) or final (conduc-

tion) states. Neglecting the Coulomb interaction, this simple formalism yields⁵

$$F_2(2x) = \frac{(2x-1)^{3/2}}{(2x)^5} \text{ for } 2x > 1. \quad (4)$$

The best fit to the data of Ref. 10 using Eqs. (3) and (4) gave $K = 3.1 \times 10^3$ in units such that E_p and E_g were in eV and β was in cm/GW, while theory gave 5.2×10^3 .⁸ When nonparabolicity was included the average β was 26% lower than theory; however, the frequency dependence of β changed very little. Interestingly, Eqs. (3) and (4) also give a fair estimate of β for a number of transparent materials measured using the third and fourth harmonics of picosecond Nd-doped yttrium-aluminum-garnet laser pulses.^{11,18}

Equations (3) and (4) pertain to a degenerate case where the two photons involved are of the same frequency and source. For a KK transformation the nondegenerate 2PA coefficient for two distinct frequencies is needed [i.e., Ω the "cause" and ω' the integration variable in Eq. (2)]. Extending the same simple model to obtain the nondegenerate 2PA coefficient has led to dispersion functions that are afflicted with "infrared divergences."^{19,20} This has been a common problem originating from the use of the $\mathbf{A} \cdot \mathbf{p}$ perturbation to calculate the bound-electronic nonlinear susceptibilities in solids.¹⁹ Although

special cases have been considered,²¹ a general theory that would rigorously address the proper scaling and spectrum of the nondegenerate 2PA is yet to be developed. For this reason we assume that the spectral function F_2 for the nondegenerate 2PA coefficient $\beta(\omega', \Omega)$ can be given by Eq. (4) modified with the substitution of $2\hbar\omega'$ by $\hbar\omega' + \hbar\Omega$; thus, $F_2(2x)$ is replaced by $F_2(x'+X)$, where $x' = \hbar\omega'/E_g$, $X = \hbar\Omega/E_g$, and $x'+X > 1$. This substitution is strictly valid only for $x'=X$; however, the predictions resulting from this substitution show remarkable agreement with the data, as will be shown.

The change of the absorption spectrum (at ω') induced by the presence of a strong pump at Ω can be written for 2PA as $\Delta\alpha(\omega'; \Omega) = \beta(\omega'; \Omega)I_\Omega$, where I_Ω denotes the irradiance of the pump field. Similarly, the change in refractive index at ω induced by the presence of a strong pump at Ω can be written as $\Delta n(\omega; \Omega) = \gamma(\omega; \Omega)I_\Omega$. Applying the KK transformation Eq. (2) at this point yields a relation between $\gamma(\omega; \Omega)$ and $\beta(\omega'; \Omega)$. Using Eq. (3) with $F_2(x'+X)$ in Eq. (2) we obtain for the degenerate case ($\omega = \Omega$),

$$\gamma = K \frac{\hbar c \sqrt{E_p}}{2n_0^2 E_g^4} G_2 \left(\frac{\hbar\omega}{E_g} \right), \quad (5)$$

where the dispersion function $G_2(x)$ is given by

$$G_2(x) = \frac{-2 + 6x - 3x^2 - x^3 - \frac{3}{4}x^4 - \frac{3}{4}x^5 + 2(1-2x)^{3/2}\Theta(1-2x)}{64x^6}, \quad (6)$$

with $\Theta(x)$ being the unit step function.

Using the value of K obtained from the 2PA measurements, $E_p = 21$ eV, and converting from γ to n_2 , we obtain the final expression for n_2 as

$$n_2(\text{esu}) = K' \frac{G_2(\hbar\omega/E_g)}{n_0 E_g^4} \quad (7)$$

where $K' = 3.4 \times 10^{-8}$ and E_g is in eV. Equation (7) explicitly shows an E_g^{-4} band-gap dependence for the magnitude of n_2 as predicted in Refs. 4 and 5, and the sign and the frequency dispersion of this quantity are given by the simple closed-form function G_2 . G_2 is the function plotted as the solid line in Fig. 1. It is important to note that no fitting parameter was used in plotting the theoretical curve and that the agreement between data and the calculation is extremely good for this wide variety of materials and large disparity in magnitudes of n_2 . A noticeable difference between the magnitude of the measured and calculated values is seen near the one-photon-absorption edge in Fig. 1. Considering the simplicity of the model in deriving Eq. (7), such deviations are not expected. The measured large negative values of n_2 as compared to the calculated values near the functional absorption edge may be attributed to the refraction due to the optical Stark effect which has been ignored in our calculations. The contribution of this mech-

anism to the electronic nonlinear susceptibility has been shown to have a strong band-gap resonance and follows the same scaling as given in Eq. (7).⁴ This effect, which is negative for all frequencies below the band gap, vanishes quickly for longer wavelengths ($\hbar\omega < E_g/2$) and gives a negligible contribution in the transparency region of the material.

The E_g^{-4} dependence of n_2 gives a variation of n_2 from 2.5×10^{-14} esu for a material such as MgF_2 at $1.06 \mu\text{m}$ to 3×10^{-10} esu for germanium at $10.6 \mu\text{m}$, which we measured using a picosecond CO_2 laser. This large variation of n_2 is better displayed by plotting n_2 scaled by n_0 and G_2 as a function of E_g on a log-log plot as shown in Fig. 2. In spite of this very large variation in magnitude of n_2 (and change in sign), this extremely simple model gives good agreement with the data for materials including both semiconductors and insulators, except very near the absorption edge. However, we must emphasize that the justification for splitting 2ω into $\omega' + \Omega$ in Eq. (4) is empirical.

In conclusion, the measured n_2 data follow a universal dispersion curve (see Fig. 1) from which values of n_2 for other materials at other wavelengths can be calculated. We have also experimentally verified the predicted band-gap scaling of n_2 . From the excellent overall agreement

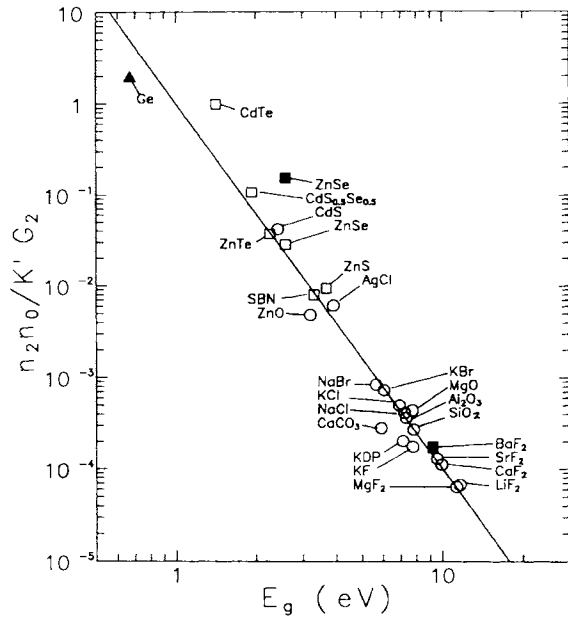


FIG. 2. A log-log plot of the data of Fig. 1 vs energy gap (E_g). Here the data are scaled by $n_0(K'G_2)^{-1}$. The solid line represents the theoretical result as obtained from Eq. (7) with no adjustable parameters and has a slope of -4 . The open circles represent the data from Ref. 6 all obtained at $\lambda = 1.06 \mu\text{m}$. The remaining data are our measurements using the Z-scan technique taken at $\lambda = 1.06 \mu\text{m}$ (open squares), at $\lambda = 0.532 \mu\text{m}$ (solid squares), and at $\lambda = 10.6 \mu\text{m}$ (solid triangle).

of the predicted magnitude and dispersion of n_2 , as calculated via the KK method, with the large number of experimental data, we conclude that the process responsible for 2PA also gives a significant if not dominant contribution to n_2 . This in turn implies that the bound-electronic nonlinear refractive index is predominantly a causal consequence of two-photon absorption just as the linear index is a causal consequence of linear absorption. This calculational approach takes advantage of the historical fact that, for the solid state, the 2PA coefficient has been calculated from a transition-rate approach.²² Thus, we have circumvented problems associated with performing a direct calculation of the third-order susceptibility.

We gratefully acknowledge the support of the National Science Foundation Grant No. ECS 8617066, U.S. Defense Advanced Research Projects Agency—Center for Night Vision and Electro-Optics, and the Florida High Technology and Industry Council. In addition, we thank

A. Miller, B. S. Wherrett, and S. Koch for useful discussions and J. Young, T. Wei, A. Said, and E. Canto for taking and analyzing portions of the n_2 data.

(a) Also with the Department of Physics.

(b) Also with the Departments of Physics and Electrical Engineering.

¹M. Sheik-Bahae, A. A. Said, T. H. Wei, D. J. Hagan, and E. W. Van Stryland, IEEE J. Quantum Electron. (to be published).

²M. Sheik-Bahae, A. A. Said, and E. W. Van Stryland, Opt. Lett. **14**, 955-957 (1989).

³D. J. Hagan, E. Canto, E. Miesak, M. J. Soileau, and E. W. Van Stryland, in *Technical Digest of the Conference on Lasers and Electro-Optics, Anaheim, CA*, Technical Digest Series Vol. 7 (Optical Society of America, Washington, DC, 1988), p. 160.

⁴B. S. Wherrett, A. C. Walker, and F. A. P. Tooley, in *Optical Nonlinearities and Instabilities in Semiconductors*, edited by H. Haug (Academic, New York, 1988), pp. 239-272.

⁵B. S. Wherrett, J. Opt. Soc. Am. B **1**, 67-72 (1984).

⁶R. Adair, L. L. Chase, and S. A. Payne, Phys. Rev. B **39**, 3337-3349 (1989).

⁷J. Callaway, *Quantum Theory of the Solid State* (Academic, New York, 1974), p. 540.

⁸M. H. Weiler, Solid State Commun. **39**, 937-940 (1981).

⁹H. S. Brandi and C. B. de Araujo, J. Phys. C **16**, 5929-5936 (1983).

¹⁰E. W. Van Stryland, M. A. Woodall, H. Vanherzeele, and M. J. Soileau, Opt. Lett. **10**, 490-492 (1985).

¹¹P. Liu, W. L. Smith, H. Lotem, J. H. Bechtel, N. Bloembergen, and R. S. Adhav, Phys. Rev. B **17**, 4620-4632 (1978).

¹²S. S. Jha and N. Bloembergen, Phys. Rev. **171**, 891-898 (1968).

¹³C. Flytzanis, Phys. Lett. **31A**, 273-274 (1970).

¹⁴J. A. Van Vechten and D. E. Aspnes, Phys. Lett. **30A**, 346-347 (1969).

¹⁵C. C. Wang, Phys. Rev. B **2**, 2045-2048 (1970).

¹⁶N. L. Boling, A. J. Glass, and A. Owyong, IEEE J. Quantum Electron. **14**, 601-608 (1978).

¹⁷D. A. B. Miller, C. T. Seaton, M. E. Prise, and S. D. Smith, Phys. Rev. Lett. **47**, 197-200 (1981).

¹⁸E. W. Van Stryland, Y. Y. Wu, D. J. Hagan, M. J. Soileau, and K. Mansour, J. Opt. Soc. Am. B **5**, 1980-1989 (1988).

¹⁹J. M. Worlock, in *Laser Handbook*, edited by F. T. Arecchi and E. D. Schulz-DuBois (North-Holland, Amsterdam, 1972), pp. 1323-1369.

²⁰G. D. Mahan, Phys. Rev. **170**, 825-838 (1968).

²¹F. V. Bunkin, Zh. Eksp. Teor. Fiz. **50**, 1685 (1966) [Sov. Phys. JETP **23**, 1121 (1966)].

²²M. Göppert-Mayer, Ann. Phys. (N.Y.) **9**, 273 (1931).